Divergent Adsorption-Dependent Luminescence of Amino-Functionalized Lanthanide Metal-Organic Frameworks for Highly Sensitive NO_2 Sensors

Arturo Gamonal,[a] Chen Sun,[a] A. Lorenzo Mariano,[b] Estefania Fernandez-Bartolome,[a] Elena SanVicente,[a] Bess Vlaisavljevich,[c] Javier Castells[d], Carlos Marti-Gastaldo[d], Roberta Poloni,*[b] Reinhold Wannemacher,*[a] Juan Cabanillas-Gonzalez*[a] and Jose Sanchez Costa*[a]

Abstract: A novel gas sensing mechanism exploiting the luminescence modulation upon NO_2 adsorption is here demonstrated. Two isostructural lanthanide based-metal-organic frameworks are used including a recognition center (amino-group) that provides high selectivity for NO_2 molecules. Energy transfer from the organic ligands to Ln is strongly dependent on the presence of NO_2, resulting in an unprecedented photo-luminescent sensing scheme. Thereby, NO_2 exposition triggers either a reversible enhancement or a decrease of the luminescence intensity, depending on the lanthanide ion (Eu or Tb). Our experimental studies combined with DFT and complete active space self-consistent field calculations, provide understanding of the nature and effects of NO_2 interactions within the MOFs and the signal transduction mechanism.

Introduction

Monitoring the emissions of toxic chemicals represents an important element in preventing and reducing pollution and in ensuring a high level of protection of the environment taken as a whole. Among the most common pollutants, nitrogen dioxide (NO_2) is a toxic gas which is generated by combustion processes at high temperatures and can cause inflammation of the airways and even death at high concentrations.[1] It also plays a pivotal role in the formation of smog and acid rain as well as being central to the formation of ground level ozone, all being associated with adverse health effects.[2] NO_2 detection is a challenging task since the majority of the commercial techniques and sensors currently used are affected by interferences, are costly or difficult to implement in the field. [3],[4],[5]

Recently, metal-organic frameworks (MOFs), have emerged as excellent candidates for chemical sensing applications.[6,7] Such porous materials can surpass some of the inherent limitations of the materials used in actual state-of-the-art sensing technologies, such as their required high temperature operating conditions, associated with a poor selectivity and high energy consumption, or their low selectivity and long response times.[8],[9] Moreover, the reticulated network of porous MOFs provides adjustable functionalities and unique optical,[10] electronic[11],[12] and magnetic[13] properties.

In this general context lanthanide-metal organic frameworks (Ln-MOFs) have attracted great interest mainly due to the large changes of their optical properties upon inclusion of analytes.[14],[15] More precisely, it has been reported that analyte hosting may alter the emission profiles and/or luminescence lifetimes of the lanthanide centre, either through enhancement, quenching or shifting of photoluminescence.[16] Furthermore, the right selection of the organic linker and its functional groups within the Ln-MOF can be used to further promote preferred guest binding for selective and sensitive detection. All this, together with their rich geometric topology, makes Ln-MOFs excellent candidates for chemosensing.[15]

In the present work three isostructural Ln-MOFs have been synthesized from 2-amino-1,4-benzene dicarboxylic acid (H_2N-BDC) and europium, terbium and gadolinium salts.[17] H_2N-BDC, already described as an antenna-like ligand in previous work,[18] also functions as an excellent recognition centre for detection of small molecules[19] such as cations and nitro-aromatics,[20] solvent molecules,[21] or even some inert gases like CO_2 or H_2.[22]

The NO_2 sensing capacity of the Ln-MOFs is studied through the changes in the luminescence intensities, resulting in divergent luminescence behavior between Tb^{+2} and Eu^{+2} based-MOF. Combining experimental studies of the adsorption/desorption of NO_2 molecules with density functional theory and multiconfigurational wave functional-based methods we show that NO_2 is bound via hydrogen bonding to the ligand leading to energy down shift of the lowest triplet state (T_1) of the photosensitizing ligand. This gas induced downshift, yields to a modulation of the energy transfer from the triplet of the ligand to the Ln ion, thus providing a powerful new approach for the design of a novel generation of divergent-luminescent sensors.

[a] Dr. A. Gamonal, C. Sun, E. Fernandez-Bartolome, E. SanVicente, Dr. R. Wannemacher,Dr. J. Cabanillas-Gonzalez, Dr. J. Sanchez Costa
IMDEA Nanociencia
Ciudad Universitaria de Cantoblanco 28049, Madrid. Spain 1
E-mail: reinhold.wannemacher@imdea.org, juan.cabanillas@imdea.org, jose.sanchezcosta@imdea.org

[b] A. L. Mariano,Dra R. Poloni
SIMaP laboratory
CNRS, University Grenoble Alpes
Grenoble. France
E-mail: roberta.poloni@grenoble-inp.fr

[c] Dra. B. Vlaisavljevich
Dep. of Chemistry
University of South Dakota
414 E Clark Street, Vermillion, SD, 57069, USA

[d] J. Castells, Prof. C. Martí Gastaldo
Instituto de Ciencia Molecular, Universitat de Valencia, Catedrático José Beltrán 2, 46980 Paterna, Spain

Supporting information for this article is given via a link at the end of the document.

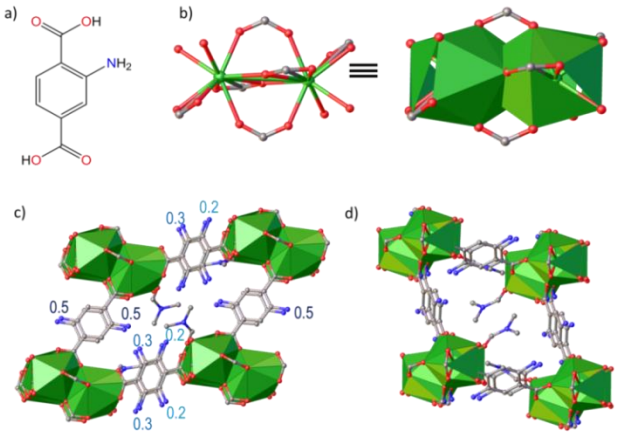

Figure 1. 2-amino-1,4-benzene dicarboxylic acid (H_2N-BDC) (a); dinuclear cluster of Ln^{3+} (in green) illustrated with balls and polyhedrons. Each metal ion is coordinated to a total of nine oxygen atoms from three chelating and two bridging N-BDC ligands, as well as from two coordinated DMF molecules (b); Ln-MOF views showing the molecular cages and the different occupancies of amino groups found by X-ray single crystal diffraction (c) and (d).

Results and Discussion

STRUCTURAL DESCRIPTION. Three porous Ln-MOFs were synthesized according the method reported by Gamez and co-authors[23], {[Tb_2(N-BDC)$_3$(DMF)$_4$] 2DMF} (**1**·2 DMF), {[Eu_2(N-BDC)$_3$(DMF)$_4$] 2DMF} (**2**·2 DMF) and [Gd_2(N-BDC)$_3$(DMF)$_4$] (**3**), see Section S2 for further details. The three crystalline-based materials grow as isostructural 3-D networks in a triclinic *P*-1 space group. The asymmetric unit contains one and one-half N-BDC ligands, one lanthanide and two coordinated DMF. Both, **1**·2DMF and **2**·2DMF, contain additional non-coordinated DMF molecules. The reported non-coordinated DMF in **1** and **2** is involved in a π-π stacking interaction with the benzene of the ligand as well as hydrogen-bonding interactions with adjacent coordinated DMF molecules (see Fig. 1 and SI for details).

PHOTOLUMINESCENCE STUDY. The photoluminescence (PL) studies of **1**, **2** and **3** were performed at room temperature as well as at liquid nitrogen temperature in the solid state, where required (see Figures S11 – S16 of the SI). The room temperature PL and PL excitation (PLE) spectra of **1**·2DMF are summarized in Figure S11a. The PL spectrum (solid green line) shows the characteristic sharp line emission from Tb^{3+} ions corresponding to $^5D_4 \rightarrow {}^7F_J$ (J = 2–6) transitions located at 642, 622, 586, 544 and 489 nm, respectively. Simultaneous emission from the ligand is manifested as a broad underlying band in the 400–550 nm range with a maximum at 445 nm. The PLE spectrum of **1** (dashed green line), obtained by monitoring the emission at 544 nm ($^5D_4 \rightarrow {}^7F_5$ transition in Tb^{3+}), exhibits a broad band due to the ligand indicating photosensitization of Tb. Regarding **2**·2DMF, the PL spectrum exhibits sharp peaks at 580, 593, 617, 651 and 697 nm assigned to $^5D_0 \rightarrow {}^7F_J$ (J = 0–4) transitions in Eu^{3+} (solid red line in Figure S11b), in agreement with previous reports.[24] Similar to the case of **1**·2DMF, the PLE spectrum monitored at 617 nm ($^5D_0 \rightarrow {}^7F_2$) exhibits a broad band covering the 300 - 450 nm range associated to the organic ligand. Concerning **3**, the PL and PLE spectra are summarized in Figure S11c. The PL spectrum (solid purple line) shows a broad band in the 400–700 nm range with a maximum at 454 nm, corresponding to the ligand emission. Note that the lowest energy level of Gd^{3+} (32200 cm^{-1}) is well above the S_1 and T_1 levels of NH_2-BDC (as confirmed below) and therefore no quenching of the ligand emission by energy transfer to Gd^{3+} occurs. The PLE spectrum of 3 (Figure S11c dashed purple line) exhibits a broad band assigned to the organic ligand.

In order to understand the Ln^{3+} sensitization mechanisms and the nature of the excited states in **1**·2DMF and **2**·2DMF**,** the S_1 and T_1 ligand energy levels were determined by PL measurements of **3**, as well as the pure ligand in solution, at 65 K (see SI for further information). Compound **3** permits the determination of the T_1 level because the lowest energy level of Gd^{3+} (32200 cm^{-1}) is well above the S_1 and T_1 levels of NH_2-BDC (as confirmed below) and therefore only phosphorescence of the ligand can be observed.

The singlet (S_1) and triplet (T_1) energy levels of the ligand were determined as the onsets of the fluorescence and phosphorescence spectra at about 405 nm (24700 cm^{-1}) and 479 nm (20900 cm^{-1}), respectively (see Figure S15 and explanation within). The energy position of T_1 with respect to the ^5D_J states of Ln^{3+} is one of the most relevant factors to determine the lanthanide luminescence efficiency in coordination compounds is the energy of T_1 with respect to the ^5D_J states of Ln^{3+}.[25] Previous studies have shown that for efficient room temperature Ln luminescence, the energy gap between the lowest T_1 energy level and the emitting state of the lanthanide ion ΔE ($^3\pi\pi^* - {}^5D_0$) should be larger than 2500 cm^{-1}.[26],[27] To ensure a fast and irreversible energy transfer. If the offset energy is lower, a back-transfer from the Ln^{3+} ion to the ligand may take place thus reducing the efficiency of the sensitized PL.

The T_1 of the ligand in **2** is located 3660 cm^{-1} above the $^5D_0$ state of Eu^{3+} (17240cm^{-1}) (see Figure 5 for further details), which confirms that back-transfer is efficiently hindered at room temperature. Conversely, the energy gap between T_1 and the emitting level of Tb^{3+} ($^5D_4$, 20430 cm^{-1}) is 470 cm^{-1}, too small to block back-transfer at room temperature, which explains the residual ligand emission in the PL spectrum of **1**[28] De-activation of Tb^{3+} levels by back-transfer to the ligand is further indicated by the significantly faster PL decay of **1** (197 μs) with respect to **2** (1.05 ms) monitored at room temperature at the respective Ln^{3+} emission peaks, (Figure S18).

NO_2 SENSING. Prior to the sensing experiment, **1** and **2** were activated by exposing them to a flow of pure synthetic air (PSA) for five minutes at room temperature, with the aim of removing the non-coordinated DMF molecules inside the lattice. This activation process was confirmed by FTIR measurements (Figure S1 and S6). Then, the samples were exposed to consecutive cycles of pure PSA and 5 ppm of NO_2 in PSA. During exposure the variation of the luminescence intensity was recorded (see SI for further details). The time duration of each cycle (5 minutes) was long enough to reach equilibrium conditions. The results for both Ln-MOF are plotted in Figure 2a-b.

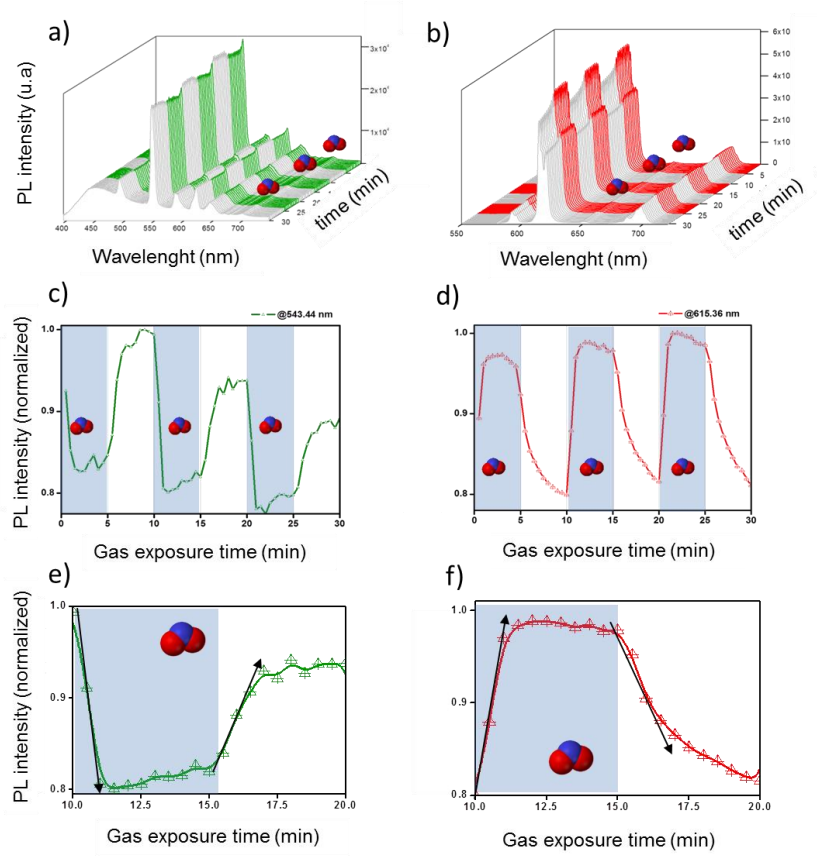

Figure 2. Evolution of PL spectra in **1** (a) and **2** (b) during three NO2 / PSA cycles. The PL intensity evolution at 543 nm for **1** (c) and at 615 nm for **2** (d) are plotted vs time (the NO2 exposition is denoted by the shaded areas). A single cycle sensing evolution illustrating the divergent behaviour for **1** (e) and **2** (f).

The exposure of **1** to 5 ppm NO_2 results in a decrease in PL intensity by about 20% monitored at the peak of the emission (543 nm) and reaching a plateau after 2 min. Subsequent exposure of **1** to PSA leads to recovery of the emission intensity within a similar time frame. Contrary to the behavior of **1**, exposure of **2** to 5 ppm of NO_2 leads to an increase in PL by about 20% during 90 seconds until it reaches a plateau. Upon PSA exposure, the PL intensity returns to the original level. Sample **2** was cycled three times in order to show the reversible behavior of the sample. In order to further assess the gas sensitivity degree, both materials were exposed to diluted NO_2 flow (from 5 to 0.5 ppm) while keeping similar measurement conditions. The results shown in Figure S17 demostrate that both samples maintain the same PL behaviour even at low pressure: the lower sensing detection with our set-up for **1** is 0.5 ppm (LOD of 1.8 ppm) and for **2**, 1 ppm (LOD of 2.2 ppm).

Importantly, exposure of **3** to NO_2 did not lead to significant changes in PL intensity, confirming that NO_2 has negligible effect on the ligand emission, this reversible change in the luminescence intensity of **1** and **2** must be associated to the NO_2 adsorption/desorption process inside the Ln-MOF.

As previously proposed for a closely-related Ln-based porous compound, the NO_2 molecule could interact within the MOF via three different mechanism; i) bonding to the metal centers,[29],[30] ii) reacting with pendant groups of the ligand,[31],[32] or iii) interacting non-covalently with the ligand.[33],[34],[35] All three options are discussed below.

Figures 2a and 2b already show no noticeable spectral shifts or changes in the crystal field splitting in the emission lines assigned to the $^5D_0 \rightarrow {}^7F_J$, J=1...4 and $^5D_4 \rightarrow {}^7F_J$, (J=2-6) transitions from either Tb^{3+} or Eu^{3+} ions, upon gas absorption. There are also no changes in the relative intensity between the specific transitions upon NO_2 uptake, although, as discussed above, the $^5D_0 \rightarrow {}^7F_2$ transition of Eu^{3+} is known to be hypersensitive to the environment, in contrast to the magnetic dipole-allowed $^5D_0 \rightarrow {}^7F_1$ transition. Furthermore, PL lifetimes measured at the respective Ln^{3+} emission peaks in **1** and **2** upon exposure to NO_2 confirm that the lifetime of **1** drops from 197 to 126 µs, whereas no significant effect of NO_2 adsorption on the PL lifetime is observed in **2** (see Figures S18 to S20). These observations strongly suggests that NO_2 adsorption does not lead to changes in the first coordination sphere around the Ln^{3+} ion.[36] Thus, a molecular absorption of NO_2 by the ligand should be expected.

AB INITIO CALCULATIONS. To understand the nature of the NO_2 interactions with the Ln-MOF, DFT calculations [37],[38–40] have been performed. A total of 8 different configurations of the NH_2 groups within the MOF were considered for **1** and **2** in order to account for the fractional occupation of the amino site reported experimentally[23] (Fig. S22). The electrostatic potential energy map of the bare MOF was computed for each configuration in order to find the NO_2 binding location.

The NO_2 molecule was placed in regions of highly attractive potential within the unit cell and a full geometrical optimization was performed (see section S11). This procedure has allowed us to correctly predict in the past the location of adsorbate CO_2 molecules within a MOF in absence of experimental guidance.[41] Remarkably, despite the fact that the starting NO_2 is near the metal site (see section S9 and Figure S25 for information), the final configuration always converges to the NO_2 being located within the pore near the NH_2 groups.

Specifically, the NO_2 binds *via* a network of hydrogen bonds, involving the amino groups of the neighbouring N-BDC ligands and CH_3 from one coordination molecule of DMF (Figure S25, S27-28 shows the NO_2 binding sites determined computationally). For both MOFs, a significant charge transfer from the ligands to NO_2 is predicted (Table S5), ranging from 0.4 to 0.7 electrons, depending on the amine configuration. This charge transfer mostly distributes on the amino groups close to the guest molecule and to a minor extent to DMF, while negligibly on the Ln ions (Table S6). The cooperative binding mechanism between samples 1 and 2 and the NO_2 molecules, attributed to multiple hydrogen bonds, electrostatics and van der Waals interactions, yield to binding energies of NO_2 ranging from 35 kJ/mol to 65 kJ/mol, depending on the specific amine configuration. This non-covalent adsorption is consistent with reversible sorption of NO_2 by the MOF. We note that binding energies (and consequently charge transfer) are determined by the specific amino group configuration, and negligibly by the specific Ln atom (Table S5).

Previous studies[27,42],[43] have shown that a modulation in the luminescence quantum yield occurs, depending on the position of the ligand triplet state (T_1) relative to the lanthanide ^5D_j levels. In order to determine whether the shift of the T_1 state of the ligand, upon binding, can explain the experimental results, multireference CASSCF/CASPT2[44] calculations were performed for the NH_2-BDC ligand bound to NO_2 (see Fig. 3c). As the NO_2 molecule is rigidly displaced from the binding configuration to larger distances from the ligand, the triplet state shifts to higher energies. The first excited triplet state, T_1, exhibits a dominant π to π* (HOMO to LUMO) character and is predicted to be at 22398 cm^{-1}(Figure S28). When the NO_2 is hydrogen bonded to the ligand the triplet is at 22137 cm^{-1} (see Figure 3b) corresponding to a downshift in energy by approximately 260 cm^{-1}. The computed downshift of T_1 as a function of the distance between NO_2 and the ligand is found to linearly correlate with the ligand-to-molecule charge transfer (see Figure S27). By making use of this linear regression and the computed charge transfer within the MOF, the T_1 downshift is estimated to be in the 230-410 cm^{-1} range, approximately, in the MOF, depending on the binding configuration.

Summarizing, the downshift of T_1, upong NO_2 adsorption, leads to opposed luminicence scenarios in **1** and **2** (see Figure 3a). The results are rationalized as follows. In **1**, the ligand T_1 level is pushed only about 200 cm^{-1} above the $^5D_4$ level of Tb^{3+} after adsorption of NO_2, leading to a detrimental effect on the PL quantum yield. The two states are close in energy and the back transfer is enhanced thus decreasing the luminescence quantum yield[45,46],[47]. Conversely, NO_2 binding in **2** results in a smaller T_1 - $^5D_1$ energy offset, (from 1900 cm^{-1} to 1640 cm^{-1}), promoting triplet-to-Eu^{3+} transfer rates as well as the total PL quantum yield.[27] These theoretical predictions are in accordance with our experimental findings.

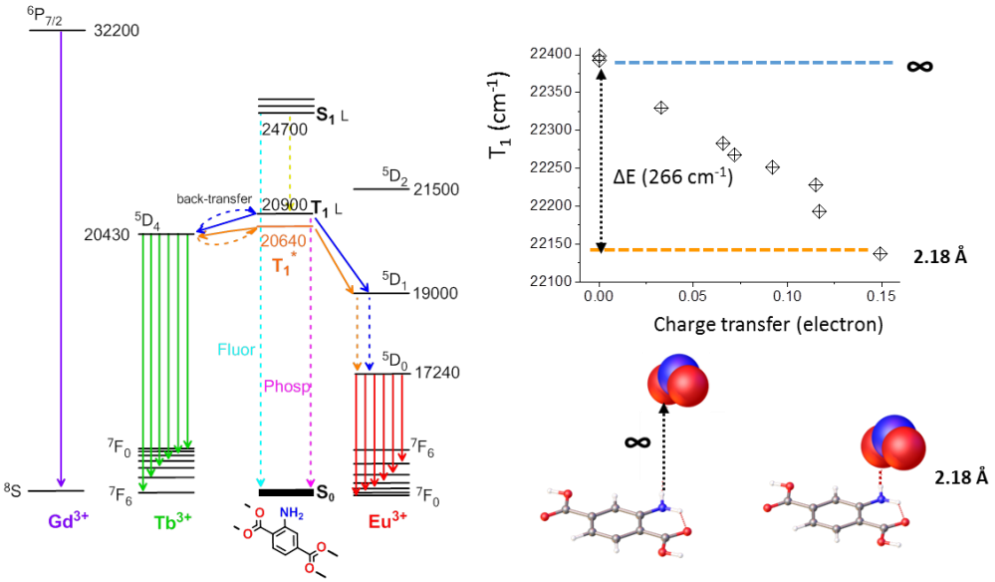

Figure 3. Jablonski diagram featuring the ground singlet (S_0), first excited singlet (S_1) and lowest triplet (T1) states of the ligand together with the relevant atomic levels of Gd^{3+}, Tb^{3+} and Eu^{3+}. Values for the energy levels are given in cm^{-1} (a). Calculated energy of T_1 vs charge transfer (b). Illustration of the ligand / NO_2 configuration used for the CASSCF/CASPT2 calculation (c).

Conclusion

We introduce a proof-of-concept sensor based on two lanthanide-based MOF that efficiently monitor (or detect), in a straightforward manner, the inclusion/exclusion of NO_2 molecules within the MOF. The reversible inclusion of NO_2 molecules in the porous framework at low concentration level triggers an increase of the intensity of the Eu^{3+} luminescence and a decrease of the Tb^{3+} luminescence intensity. Experimental spectroscopy and computational studies were combined to deliver the signal transduction mechanism. Based on the divergent luminescence change upon NO_2 exposure in **1** and **2**, the lack of changes in the relative intensities of the $^5D_J \rightarrow {}^7F_J$ transitions, and the computational predictions we conclude that the modification of the luminescence intensity can be ascribed to changes in the relative positions of the ligand triplet and the Ln energy levels upon NO_2 adsorption. In spite of the weak interaction (physisorption) between NO_2 and the MOF, the affinity of the amino groups for NO_2 makes this MOF sensitive enough for detection of NO_2 in conventional luminescence displays without requiring expensive electronics. This study herein suggests a powerful new approach for the design of future luminescent sensors of noxious volatile compounds.

Experimental Section

Experimental Details. Compounds **1**, **2** and **3** were synthesized according to the literature procedures (see S1-S2). TGA, FT-IR, PXPD are detailed in S3 to S5. Photo-luminescence measurements, sorption measurements and Ab initio calculation details are also described in S6 to S11 sections.

Acknowledgements

JSC is grateful to the Spanish MINECO for financial support through National Research Project (CTQ2016-80635-P), the Ramon y Cajal Research program (RYC-2014-16866) and the Comunidad Autónoma de Madrid (PEJD-2017-PRE/IND-4037) for funding support. IMDEA Nanociencia acknowledges support from the 'Severo Ochoa' Programme for Centres of Excellence in R&D (MINECO, Grant SEV-2016-0686). This research used resources of the Advanced Light Source, which is a DOE Office of Science User Facility under contract no. DE-AC02-05CH11231. We would like to thank to XALOC-ALBA synchrotron source under the project no. (2018012561). JC-G and RW acknowledge funding from the European Union structural funds and the Comunidad de Madrid MAD2D-CM (S2013/MIT-3007) and NMAT2D-CM (S2018/NMT-4511) projects. JC-G acknowledges funding from MINECO through projects RTI2018-097508-B-I00 (AMAPOLA) and PCIN-2015-169-C02-01/02. RW acknowledges funding from MINECO through project MAT2015-71879-P. IMDEA Nanociencia acknowledges support from the “Severo Ochoa” Programme for Centres of Excellence in R&D (MINECO, Grant SEV-2016-0686). Computational resources were granted by GENCI under CINES grant A0060907211 and by froggy platform of the CIMENT infrastructure. This work benefited from the support of the project ANR-15-CE06-0003-01 funded by the French National Agency for Research.

Keywords: Lanthanide Metal-Organic Framework • NO_2 sensing • Divergent luminescent behaviour• DFT calculations

[1] K. G. Sexton, H. E. Jeffries, M. Jang, R. M. Kamens, M. Doyle, I. Voicu, I. Jaspers, *Inhal. Toxicol.* **2004**, *16*, 107–114.

[2] M. E. Jenkin, S. R. Utembe, R. G. Derwent, *Atmos. Environ.* **2008**, *42*, 323–336.

[3] T. C. Brueggemann, M.-D. Przybylski, S. P. Balaji, F. J. Keil, *J. Phys. Chem. C* **2010**, *114*, 6567–6587.

[4] K. Smith, S. Almeer, S. J. Black, *Chem. Commun.* **2000**, 1571–1572.

[5] J. O. Petunchi, W. K. Hall, *Appl. Catal. B, Environ.* **1993**, *2*, 17–26.

[6] X. Fang, B. Zong, S. Mao, *Nano-Micro Lett.* **2018**, *10*, 1–19.

[7] L. E. Kreno, K. Leong, O. K. Farha, M. Allendorf, R. P. Van Duyne, J. T. Hupp, *Chem. Rev.* **2012**, *112*, 1105–1125.

[8] J. Kong, N. R. Franklin, C. Zhou, M. G. Chapline, S. Peng, K. Cho, H. Dai, *Science.* **2000**, *287*, 622–625.

[9] S. Cui, H. Pu, S. A. Wells, Z. Wen, S. Mao, J. Chang, M. C. Hersam, J. Chen, *Nat. Commun.* **2015**, *6*, 8632_1-8632_9.

[10] J. Cornelio, T. Y. Zhou, A. Alkaş, S. G. Telfer, *J. Am. Chem. Soc.* **2018**, *140*, 15470–15476.

[11] S. S. Park, E. R. Hontz, L. Sun, C. H. Hendon, A. Walsh, T. Van Voorhis, M. Dincə, *J. Am. Chem. Soc.* **2015**, *137*, 1774–1777.

[12] E. A. Dolgopolova, V. A. Galitskiy, C. R. Martin, H. N. Gregory, B. J. Yarbrough, A. M. Rice, A. A. Berseneva, O. A. Ejegbavwo, K. S. Stephenson, P. Kittikhunnatham, S.G. Karakalos, M.D. Smith, A. Greytak, S. Garashchuk, N.B. Shustova, *J. Am. Chem. Soc.* **2019**, *141*, 5350–5358.

[13] G. Mínguez Espallargas, E. Coronado, *Chem. Soc. Rev.* **2018**, *47*, 533–557.

[14] H. Xu, C. S. Cao, X. M. Kang, B. Zhao, *Dalton Trans.* **2016**, *45*, 18003–18017.

[15] Z. Hu, B. J. Deibert, J. Li, *Chem. Soc. Rev.* **2014**, *43*, 5815–5840.

[16] Y. Su, J. Yu, Y. Li, S. F. Z. Phua, G. Liu, W. Q. Lim, X. Yang, R. Ganguly, C. Dang, C. Yang, et al., *Commun. Chem.* **2018**, *1*, 12_1-12_13.

[17] J. S. Costa, P. Gamez, C. A. Black, O. Roubeau, S. J. Teat, J. Reedijk, *Eur. J. Inorg. Chem.* **2008**, 1551–1554.

[18] Y. Yang, R. Lin, L. Ge, L. Hou, P. Bernhardt, T. E. Rufford, S. Wang, V. Rudolph, Y. Wang, Z. Zhu, *Dalton Trans.* **2015**, *44*, 8190–8197.

[19] J. N. Hao, B. Yan, *J. Mater. Chem. C* **2014**, *2*, 6758–6764.

[20] E. J. Kyprianidou, T. Lazarides, S. Kaziannis, C. Kosmidis, G. Itskos, M. J. Manos, A. J. Tasiopoulos, *J. Mater. Chem. A* **2014**, *2*, 5258–5266.

[21] X. Y. Xu, B. Yan, *ACS Appl. Mater. Interfaces* **2015**, *7*, 721–729.

[22] X. Si, C. Jiao, F. Li, J. Zhang, S. Wang, S. Liu, Z. Li, L. Sun, F. Xu, Z. Gabelica, et al., *Energy Environ. Sci.* **2011**, *4*, 4522–4527.

[23] C. A. Black, J. S. Costa, W. T. Fu, C. Massera, O. Roubeau, S. J. Teat, G. Aromı, P. Gamez, J. Reedijk, *Inorg. Chem.* **2009**, *48*, 1062–1068.

[24] K. Binnemans, *Coord. Chem. Rev.* **2015**, *295*, 1–45.

[25] C. Binnemans, Koen ; Görller-Walrand, *J. Rare Earths* **1996**, *14*, 173–180.

[26] S. F. Mason, B. Stewart, *Mol. Phys.* **1985**, *55*, 611–620.

[27] G. R. Choppin, R. L. Fellows, *Coord. Chem. Rev.* **1976**, *18*, 199–224.

[28] G. Blasse, in *Spectra and Chemical Interactions. Structure and*

Bonding,*Vol 26* (Ed.: R.J.P. Williams),Springer, Berlin, Heidelberg, **1976**, pp. 43–79.

[29] Susumu Sato and Masanobu Wada, *Bull. Chem. Soc. Jpn.* **1970**, *43*, 1955–1962.

[30] C. D. M. Donega, E. F. Silva, G. F. de Sá, O. L. Malta, R. L. Longo, P. A. Santa-Cruz, *Coord. Chem. Rev.* **2000**, *196*, 165–195.

[31] M. Latva, H. Takalob, V. M. Mukkala, C. Matachescu, J. C. Rodríguez-Ubis, J. Kankare, *J. Lumin.* **1997**, *75*, 149–169.

[32] L. Smentek, A. Ke˛dziorski, *J. Lumin.* **2010**, *130*, 1154–1159.

[33] K. I. Hadjiivanov, *Catal. Rev. - Sci. Eng.* **2000**, *42*, 71–144.

[34] K. I. Hadjiivanov, *Microporous Mesoporous Mater.* **1998**, *24*, 41–49.

[35] A. M. Ebrahim, B. Levasseur, T. J. Bandosz, *Langmuir* **2013**, *29*, 168–174.

[36] B. Levasseur, A. M. Ebrahim, T. J. Bandosz, *Langmuir* **2012**, *28*, 5703–5714.

[37] G. W. Peterson, J. J. Mahle, J. B. DeCoste, W. O. Gordon, J. A. Rossin, *Angew. Chemie Int. Ed.* **2016**, *55*, 6235–6238.

[38] J. N. Hao, B. Yan, *Nanoscale* **2016**, *8*, 2881–2886.

[39] Y. L. Zhao, S. L. Garrison, C. Gonzalez, W. D. Thweatt, M. Marquez, *J. Phys. Chem. A* **2007**, *111*, 2200–2205.

[40] G. R. Choppin, D. R. Peterman, *Coord. Chem. Rev.* **1998**, *174*, 283–299.

[41] P. Giannozzi, S. Baroni, N. Bonini, M. Calandra, R. Car, C. Cavazzoni, D. Ceresoli, G. L. Chiarotti, M. Cococcioni, I. Dabo, A. Dal Corso,S. De Gironcoli, S. Fabris, G. Fratesi, R. Gebauer, U. Gerstmann, C. Gougoussis, A. Kokalj, M. Lazzeri, L. Martin-Samos, N Marzari, F. Mauri, R. Mazzarello, S. Paolini, A. Pasquarello, L. Paulatto, C. Sbraccia, S. Scandolo, G. Sclauzero, A.P. Seitsonen, A. Smogunov, P. Umari, R.M. Wentzcovitch., **2009**, DOI 10.1088/0953-8984/21/39/395502.

[42] M. Dion, H. Rydberg, E. Schroder, D. C. Langreth, B. I. Lundqvist, **2004**, *1*, 22–25.

[43] K. Lee, É. D. Murray, L. Kong, B. I. Lundqvist, D. C. Langreth, *Phys. Rev. B - Condens. Matter Mater. Phys.* **2010**, *82*, 3–6.

[44] I. Hamada, *Phys. Rev. B* **2014**, *89*, 121103-1–121103-5.

[45] R. Poloni, B. Smit, J. B. Neaton, *J. Am. Chem. Soc.* **2012**, *134*, 6714–6719.

[46] R. D. Archer, H. Chen, L. C. Thompson, *Inorg. Chem.* **2002**, *37*, 2089–2095.

[47] N. Arnaud, J. Georges, *Spectrochim. Acta - Part A Mol. Biomol. Spectrosc.* **2003**, *59*, 1829–1840.

[48] T. Shiozaki, *Wiley Interdiscip. Rev. Comput. Mol. Sci.* **2018**, *8*, 1–7.

[49] S. Omagari, T. Nakanishi, T. Seki, Y. Kitagawa, Y. Takahata, K. Fushimi, H. Ito, Y. Hasegawa, *J. Phys. Chem. A* **2015**, *119*, 1943–1947.

[50] S. Omagari, T. Nakanishi, Y. Kitagawa, T. Seki, K. Fushimi, H. Ito, A. Meijerink, Y. Hasegawa, *Sci. Rep.* **2016**, *6*, 1–11.

[51] S. Katagiri, Y. Tsukahara, Y. Hasegawa, Y. Wada, *Bull. Chem. Soc. Jpn.* **2007**, *80*, 1492–1503.

Supramolecular interactions are key for highly sensitive detection of NO2 using porous amino-linked lanthanide metal-organic framework. Tuning of ligand-to-metal energy transfer causes an unprecendented divergent luminescence response to NO2 sorption in Ln-MOFs rationalized using computational and photoluminescence method

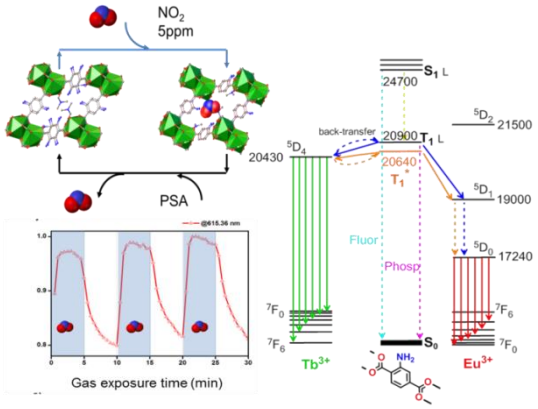

A. Gamonal, C. Sun, A. L. Mariano, E. Fernandez-Bartolome, E. SanVicente, B. Vlaisavljevich, R. Poloni, R. Wannemacher,* J. Cabanillas-Gonzalez* and J. Sanchez Costa**

Page No. – Page No.

Title